

# Optimal SNR Analysis for Single-user RIS Systems

Ikram Singh\*, Peter J. Smith†, Pawel A. Dmochowski\*

\*School of Engineering and Computer Science, Victoria University of Wellington, Wellington, New Zealand

†School of Mathematics and Statistics, Victoria University of Wellington, Wellington, New Zealand

email: {ikram.singh,peter.smith,pawel.dmochowski}@ecs.vuw.ac.nz

**Abstract**—In this paper, we present an analysis of the optimal uplink SNR of a SIMO RIS-aided wireless link. We assume that the channel between base station and RIS is a rank-1 LOS channel while the user-RIS and user-base station channels are correlated Rayleigh. We derive an exact closed form expression for the mean SNR and an approximation for the SNR variance leading to an accurate gamma approximation to the distribution of the UL SNR. Furthermore, we analytically characterise the effects of correlation on SNR, showing that correlation in the user-base station channel can have negative effects on the mean SNR, while correlation in the user-RIS channel improves system performance. For systems with a large number of RIS elements, this improvement saturates to a gain of approximately 27.32%.

## I. INTRODUCTION

Reconfigurable Intelligent Surface (RIS) aided wireless networks are currently the subject of considerable research attention due to their ability to manipulate the channel between users (UEs) and base station (BS) via the RIS. Assuming that channel state information (CSI) is known at the RIS, one can intelligently alter the RIS phases, essentially changing the channel, to improve various aspects of system performance. Here, we focus on a single user system and assume the common system scenario where a RIS is carefully located near the BS such that a rank-1 Line-of-Sight (LOS) channel is formed between the BS and RIS.

System scenarios with a LOS channel from BS to RIS are also considered in [1]–[6] with motivation for the LOS assumption given in [3], [6]. All of these existing works aim to enhance the system to achieve some optimal system performance (Sum Rate, SINR, etc.) by tuning the RIS phases. In particular, [3] gives a closed form RIS phase solution without the presence of a direct UE-BS channel for a single user setting while [5] gives a closed form phase solution with the presence of a direct channel. However, once the optimal RIS has been defined there is no analysis regarding the impact of correlation on the resulting performance in [1]–[6].

For the RIS to UE and the direct BS to UE links, scattered channels are a reasonable assumption and spatial correlation in the channels is an important factor, especially at the RIS where small inter-element spacing may be envisaged. Several papers do consider spatial correlation in the small-scale fading channels [3], [4], [6]–[8]. However, these papers are simulation based and no analysis of correlation impact is given.

In [9]–[12], some analysis is provided into the statistical properties of the channel. In particular, [9], [10], [12] provide a closed form expression for the mean SNR in the absence of a UE-BS channel with [12] providing a PDF and CDF for

the mean SNR. In [10], [11], an upper bound is given for the ergodic capacity. However, [9]–[12] do not consider correlated fading channels.

Hence, in this paper, we focus on an analysis of the optimal uplink (UL) SNR for a single user RIS aided link with a rank-1 LOS RIS-BS channel and correlated Rayleigh fading for the UE-BS and UE-RIS channels. In particular, for this system and channel model we make the following contributions:

- An exact closed-form result for  $\mathbb{E}\{\text{SNR}\}$  and an approximate closed form expression for  $\text{Var}\{\text{SNR}\}$  are derived. These are used to show that a gamma distribution provides a good approximation of the UL optimal SNR distribution.
- Exact closed-form expressions for both  $\mathbb{E}\{\text{SNR}\}$  and  $\text{Var}\{\text{SNR}\}$  are derived for uncorrelated Rayleigh channels and presented as a special case.
- The analysis is leveraged to gain insight into the impact of spatial correlation and system dimension on the mean SNR. We prove that correlation in the UE-BS channel can have negative effects, while correlation in the UE-RIS channel improves system performance. For systems with a large number of RIS elements, this improvement saturates to a relative gain of approximately 27.32%.

*Notation:*  $\mathbb{E}\{\cdot\}$  represents statistical expectation.  $\Re\{\cdot\}$  is the Real operator.  $\|\cdot\|_2$  denotes the  $\ell_2$  norm. Upper and lower boldface letters represent matrices and vectors respectively.  $\mathcal{CN}(\boldsymbol{\mu}, \mathbf{Q})$  denotes a complex Gaussian distribution with mean  $\boldsymbol{\mu}$  and covariance matrix  $\mathbf{Q}$ .  $\mathcal{U}[a, b]$  denotes a uniform random variable taking on values between  $a$  and  $b$ .  $\chi_k^2$  denotes a chi square distribution with  $k$  degrees of freedom.  $\mathbf{1}_n$  represents an  $n \times n$  matrix with unit entries. The transpose and Hermitian transpose operators are denoted as  $(\cdot)^T$ ,  $(\cdot)^H$  respectively. The trace and diagonal operators are denoted by  $\text{tr}\{\cdot\}$  and  $\text{diag}\{\cdot\}$  respectively. The angle of a vector  $\mathbf{x}$  of length  $N$  is defined as  $\angle \mathbf{x} = [\angle x_1, \dots, \angle x_N]^T$  and the exponent of a vector is defined as  $e^{\mathbf{x}} = [e^{x_1}, \dots, e^{x_N}]^T$ .

## II. SYSTEM MODEL

As shown in Fig. 1, we examine a RIS aided single user single input multiple output (SIMO) system where a RIS with  $N$  reflective elements is located close to a BS with  $M$  antennas such that a rank-1 LOS condition is achieved between the RIS and BS.

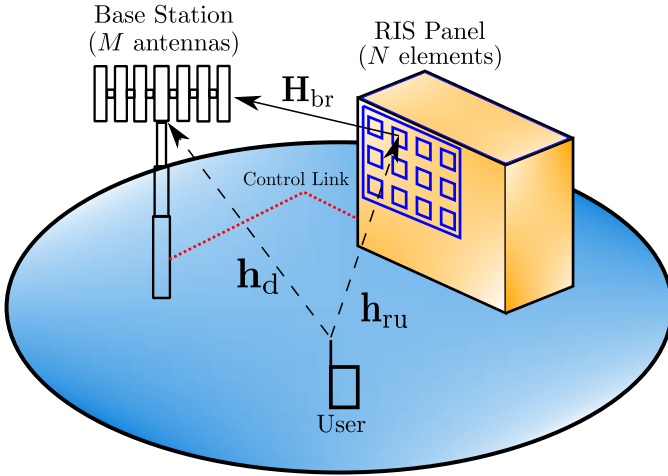


Fig. 1: System model where the red dashed line is the control link for the RIS phases.

### A. Channel Model

Let  $\mathbf{h}_d \in \mathbb{C}^{M \times 1}$ ,  $\mathbf{h}_{ru} \in \mathbb{C}^{N \times 1}$ ,  $\mathbf{H}_{br} \in \mathbb{C}^{M \times N}$  be the UE-BS, UE-RIS and RIS-BS channels, respectively. The diagonal matrix  $\Phi \in \mathbb{C}^{N \times N}$ , where  $\Phi_{r,r} = e^{j\phi_r}$  for  $r = 1, 2, \dots, N$ , contains the reflection coefficients for each RIS element. The global UL channel is thus represented by

$$\mathbf{h} = \mathbf{h}_d + \mathbf{H}_{br} \Phi \mathbf{h}_{ru}. \quad (1)$$

In the channel model, we consider the correlated Rayleigh channels:  $\mathbf{h}_d = \sqrt{\beta_d} \mathbf{R}_d^{1/2} \mathbf{u}_d$  and  $\mathbf{h}_{ru} = \sqrt{\beta_{ru}} \mathbf{R}_{ru}^{1/2} \mathbf{u}_{ru} \triangleq \sqrt{\beta_{ru}} \tilde{\mathbf{h}}_{ru}$  where  $\beta_d$  and  $\beta_{ru}$  are the link gains,  $\mathbf{R}_d, \mathbf{R}_{ru}$  are the correlation matrices for UE-BS and UE-RIS links respectively and  $\mathbf{u}_d, \mathbf{u}_{ru} \sim \mathcal{CN}(\mathbf{0}, \mathbf{I})$ . The rank-1 LOS channel from RIS to BS has link gain  $\beta_{br}$  and is given by  $\mathbf{H}_{br} = \sqrt{\beta_{br}} \mathbf{a}_b \mathbf{a}_r^H$  where  $\mathbf{a}_b$  and  $\mathbf{a}_r$  are arbitrary steering vectors at the BS and RIS respectively. Particular examples of steering vectors for a Vertical Uniform Rectangular Array (VURA) are defined in Sec. V.

The link gains are modeled by the classical path-loss and shadowing model,

$$\beta_{br} = d_{br}^{-2}, \beta_{ru} = A_0 L \left( \frac{d_{ru}}{d_0} \right)^{-\gamma}, \beta_d = A_0 L \left( \frac{d_d}{d_0} \right)^{-\gamma} \quad (2)$$

where  $A_0$  is the received power at reference distance  $d_0$  in the absence of shadowing.  $d_{br}, d_{ru}$  and  $d_d$  are the distances between the RIS-BS, UE-RIS and UE-BS respectively.  $\gamma$  is the pathloss exponent and  $L$  represents lognormal shadowing with standard deviation  $\sigma_{sf}$  dB.

The correlation matrices are defined by the well-known model where the correlation decays exponentially with antenna separation, Hence,

$$(\mathbf{R}_{ru})_{ik} = \rho_{ru}^{\frac{d_{i,k}}{d_b}}, \quad (\mathbf{R}_d)_{ik} = \rho_d^{\frac{d_{i,k}}{d_r}} \quad (3)$$

where  $0 < \rho_{ru} < 1$ ,  $0 < \rho_d < 1$ .  $d_{i,k}$  is the distance between the  $i^{\text{th}}$  and  $k^{\text{th}}$  antennas/elements at the BS/RIS.  $d_b$  and  $d_r$  are

the nearest-neighbour BS antenna separation and RIS element separation, respectively, which are measured in wavelength units.

### B. Optimal SNR

Using (1), the received signal at the BS is,

$$\mathbf{r} = (\mathbf{h}_d + \mathbf{H}_{br} \Phi \mathbf{h}_{ru}) s + \mathbf{n} = \mathbf{h} s + \mathbf{n}, \quad (4)$$

where  $s$  is the transmitted signal with power  $E_s$  and  $\mathbf{n} \sim \mathcal{CN}(\mathbf{0}, \sigma^2 \mathbf{I})$ . For a single user, Matched Filtering (MF) is the optimal combining method so the optimal UL SNR is,

$$\text{SNR} = \mathbf{h}^H \mathbf{h} \bar{\tau}, \quad (5)$$

where  $\bar{\tau} = \frac{E_s}{\sigma^2}$ . The optimal RIS phase matrix to maximize (5) can be computed using the main steps outlined in [5, Sec. III-B] but using an UL channel model instead of downlink. Substituting the channel vectors and through some matrix algebraic manipulation, the optimal RIS phase matrix is,

$$\Phi = \frac{\mathbf{a}_b^H \mathbf{h}_d}{|\mathbf{a}_b^H \mathbf{h}_d|} \text{diag}\{e^{j\angle \mathbf{a}_r}\} \text{diag}\{e^{-j\angle \mathbf{h}_{ru}}\}. \quad (6)$$

Substituting (6) into  $\mathbf{h}$ , the optimal UL global channel is,

$$\mathbf{h} = \mathbf{h}_d + \sqrt{\beta_{br} \beta_{ru}} \psi \sum_{n=1}^N \left| \tilde{\mathbf{h}}_{ru,n} \right| \mathbf{a}_b, \quad (7)$$

where  $\psi = \frac{\mathbf{a}_b^H \mathbf{h}_d}{|\mathbf{a}_b^H \mathbf{h}_d|}$ . Hence, the optimal UL SNR is

$$\text{SNR} = (\mathbf{h}_d^H + \alpha^* \mathbf{a}_b^H) (\mathbf{h}_d + \alpha \mathbf{a}_b) \bar{\tau}, \quad (8)$$

where  $\alpha = \sqrt{\beta_{br} \beta_{ru}} \psi \sum_{n=1}^N \left| \tilde{\mathbf{h}}_{ru,n} \right|$ .

## III. $\mathbb{E}\{\text{SNR}\}$ AND $\text{VAR}\{\text{SNR}\}$

### A. Correlated Rayleigh Case

Here, we provide an exact closed form expression for  $\mathbb{E}\{\text{SNR}\}$  and a closed form approximation for  $\text{Var}\{\text{SNR}\}$ .

**Theorem 1.** The mean SNR is given by

$$\left( \beta_d M + \frac{N A \pi}{2} \sqrt{\beta_d \beta_{br} \beta_{ru}} + \beta_{br} \beta_{ru} M(N+F) \right) \bar{\tau}, \quad (9)$$

with  $F$  given by

$$F = \sum_{i=1}^N \sum_{\substack{j=1 \\ i \neq j}}^N \frac{\pi}{4} \left( 1 - |\rho_{ij}|^2 \right)^2 {}_2F_1 \left( \frac{3}{2}, \frac{3}{2}; 1; |\rho_{ij}|^2 \right), \quad (10)$$

and  $A = \left\| \mathbf{R}_d^{1/2} \mathbf{a}_b \right\|_2$ , where  ${}_2F_1(\cdot)$  is the Gaussian hypergeometric function and  $\rho_{ij} = (\mathbf{R}_{ru})_{ij}$ .

*Proof.* See Appendix A for the derivation of (9). ■

In the calculation of  $\text{Var}\{\text{SNR}\}$ , all terms are derived exactly except for the 3<sup>rd</sup> and 4<sup>th</sup> moments of  $Y = \sum_{n=1}^N \left| \tilde{\mathbf{h}}_{ru,n} \right|$ , as these moments, to the best of the authors' knowledge, are intractable. Noting that  $Y$  is positive and

unimodal and motivated by the work in [10], we approximate the distribution of  $Y$  with a gamma distribution. This gives the following result:

**Result.** An approximation for  $\text{Var}\{\text{SNR}\}$  is given by

$$\begin{aligned} & \left( \beta_d^2 \text{tr}\{\mathbf{R}_d^2\} + \beta_d^{3/2} \sqrt{\beta_{br}\beta_{ru}} N\pi(B - MA) \right. \\ & + \beta_d \beta_{br} \beta_{ru} A^2 \left( 4(N + F) - \frac{N^2 \pi^2}{4} \right) \\ & + MA \sqrt{\beta_d} (\beta_{br} \beta_{ru})^{3/2} (2\sqrt{\pi} C_1 - N(N + F)\pi) \\ & \left. + (M\beta_{br}\beta_{ru})^2 (C_2 - (N + F)^2) \right) \bar{\tau}^2 \end{aligned} \quad (11)$$

where  $B = MA + \mathbf{a}_b^H \mathbf{R}_d^2 \mathbf{a}_b / 2A$ ,  $C_1 = b^3 a \prod_{k=1}^2 (k + a)$ ,  $C_2 = b^4 a \prod_{k=1}^3 (k + a)$ ,

$$a = \frac{N^2 \pi}{4(N + F) - N^2 \pi}, \quad b = \frac{2}{N\sqrt{\pi}} \left( N + F - \frac{N^2 \pi}{4} \right),$$

$F$  is given by (10) and  $A$  is given in Theorem 1.

*Proof.* See Appendix B for the derivation of (11). ■

### B. Special Case: Uncorrelated Rayleigh Case

For independent Rayleigh fading, we provide exact closed form expressions for both  $\mathbb{E}\{\text{SNR}\}$  and  $\text{Var}\{\text{SNR}\}$ . Here,  $\mathbf{h}_d, \mathbf{h}_{ru} \sim \mathcal{CN}(\mathbf{0}, \mathbf{I})$  (i.e.  $\mathbf{R}_d = \mathbf{I}_M$  and  $\mathbf{R}_{ru} = \mathbf{I}_N$ ). As such, (10) simplifies to

$$F_u = \sum_{i=1}^N \sum_{\substack{j=1 \\ i \neq j}}^N \frac{\pi}{4} = N(N-1) \frac{\pi}{4}. \quad (12)$$

From  $\|\mathbf{a}_b\|_2 = \sqrt{M}$ , the value of  $\mathbb{E}\{\text{SNR}\}$  for uncorrelated channels is,

$$\left( \beta_d M + \frac{\sqrt{M} N \pi}{2} \sqrt{\beta_d \beta_{br} \beta_{ru}} + \beta_{br} \beta_{ru} M(N + F_u) \right) \bar{\tau}. \quad (13)$$

Furthermore an exact expression for  $\text{Var}\{\text{SNR}\}$  is given by

$$\begin{aligned} & \left( \beta_d^2 M + \beta_d^{3/2} \sqrt{\beta_{br}\beta_{ru}} N\pi(B_u - 2M^{3/2}) \right. \\ & + \beta_d \beta_{br} \beta_{ru} M \left( 4(N + F_u) - \frac{N^2 \pi^2}{4} \right) \\ & + M^{3/2} \sqrt{\beta_d} (\beta_{br} \beta_{ru})^{3/2} (2\sqrt{\pi} C_{u1} - N(N + F_u)\pi) \\ & \left. + (M\beta_{br}\beta_{ru})^2 (C_{u2} - (N + F_u)^2) \right) \bar{\tau}^2, \end{aligned} \quad (14)$$

with

$$\begin{aligned} B_u &= M^{3/2} + \frac{1}{2} \sqrt{M} \\ C_{u1} &= \frac{N\sqrt{\pi}}{2} \left( \frac{\pi}{4} \prod_{k=1}^2 (N - k) + 3N - \frac{3}{2} \right) \\ C_{u2} &= 2N + \binom{N}{2} \left( \prod_{k=2}^3 (N - k) \frac{\pi^2}{8} + 6 + 3\pi(N - 1) \right) \end{aligned}$$

where  $F_u$  is given by (12) and  $C_{u1}$ ,  $C_{u2}$  are derived in Appendix D.

### IV. PERFORMANCE INSIGHTS BASED ON $\mathbb{E}\{\text{SNR}\}$

Here, we present an analysis of  $\mathbb{E}\{\text{SNR}\}$  in Sec. III with respect to the correlation levels  $\rho_{ru}, \rho_d$  and give asymptotic results for large numbers of RIS elements (large  $N$ ).

#### A. Effect of $\rho_{ru}$ on $\mathbb{E}\{\text{SNR}\}$

With respect to the correlation level  $\rho_{ru}$ , (9) can be lower and upper bounded due to  $F$  being monotonic in  $\rho_{ru}$ . The upper bound for (10) as  $\rho_{ru} \rightarrow 1$  is

$$F_{UB} \stackrel{(a)}{=} \sum_{i=1}^N \sum_{\substack{j=1 \\ i \neq j}}^N \frac{\pi}{4} {}_2F_1 \left( -\frac{1}{2}, -\frac{1}{2}, 1; 1 \right) \stackrel{(b)}{=} N(N-1), \quad (15)$$

where (a) uses [13, Eq. (15.3.3)] to perform a linear transformation of the hypergeometric function and (b) uses [13, Eq. (15.1.20)] to reduce the hypergeometric function to a known value along with evaluation of the double summation. Using (12) and (15), (10) has the following upper and lower bounds,

$$F_u = N(N-1) \frac{\pi}{4} \leq F \leq N(N-1). \quad (16)$$

This means that the upper and lower bounds for SNR with respect to  $\rho_{ru}$  are

$$\mathbb{E}\{\text{SNR}\}_{UB} = \left( \beta_d M + \frac{NA\pi}{2} \sqrt{\beta_d \beta_{br} \beta_{ru}} + \beta_{br} \beta_{ru} MN^2 \right) \bar{\tau}, \quad (17)$$

$$\mathbb{E}\{\text{SNR}\}_{LB} =$$

$$\left( \beta_d M + \frac{NA\pi}{2} \sqrt{\beta_d \beta_{br} \beta_{ru}} + \beta_{br} \beta_{ru} M(N + F_u) \right) \bar{\tau}. \quad (18)$$

Hence, correlation in  $\mathbf{h}_{ru}$  improves the mean SNR. From (17) and (18) we observe that the first term in  $\mathbb{E}\{\text{SNR}\}$  is of order  $M$  and the third term is of order  $MN^2$ . In Sec. IV-B we show that the second term has a maximum order of  $MN$ . Hence, the third term is dominant giving  $\mathbb{E}\{\text{SNR}\} = \mathcal{O}(MN^2)$  and the largest channel effect will be an increase in SNR due to correlation at the RIS.

#### B. Effect of $\rho_d$ on $\mathbb{E}\{\text{SNR}\}$

The only variable in (9) that is affected by  $\rho_d$  is  $A$ . As  $\rho_d \rightarrow 0$ ,  $A \rightarrow \sqrt{M}$ . As  $\rho_d \rightarrow 1$ ,  $\mathbf{R}_d \rightarrow \mathbf{1}_M$  which means that

$$A = \left\| \mathbf{R}_d^{1/2} \mathbf{a}_b \right\|_2 \rightarrow \frac{1}{\sqrt{M}} \left\| \mathbf{1}_M \mathbf{a}_b \right\|_2 = \left| \sum_{i=1}^M \mathbf{a}_{b,i} \right| \leq M.$$

Hence, the second term in (9) has a maximum order of  $MN$  as stated above. Although the maximum order can be achieved with perfect correlation ( $\rho_d = 1$ ), for typical environments the value of  $A$  tends to reduce as correlation is increased. To explain this property we show via an example based on a uniform linear array (ULA) that for highly correlated BS antennas,  $\sqrt{M}$  tends to be larger than  $\left| \sum_{i=1}^M \mathbf{a}_{b,i} \right|$  for large  $M$ . For a ULA, ignoring elevation angles, the steering vector elements can be given by  $\mathbf{a}_{b,i} = e^{j2\pi(i-1)d_b \sin(\theta)}$  where  $\theta$  is the azimuth angle of arrival at the BS. Here,

$$\left| \sum_{i=1}^M \mathbf{a}_{b,i} \right| = \left| \frac{1 - e^{j2M\pi d_b \sin(\theta)}}{1 - e^{j2\pi d_b \sin(\theta)}} \right| = \left| \frac{\sin(M\pi d_b \sin(\theta))}{\sin(\pi d_b \sin(\theta))} \right|.$$

This well-known sinusoidal ratio is much smaller than  $\sqrt{M}$  for large  $M$  as long as  $\theta$  is not arbitrarily close to zero. Therefore, systems with a large number of BS antennas can expect greater system performance when  $\mathbf{h}_d$  is uncorrelated unless the RIS-BS link is extremely close to broadside.

In summary, high correlation at the RIS and low correlation at the BS tend to be beneficial and we refer to this scenario as the *favorable channel scenario*.

### C. Favorable Channel Scenario and Asymptotic Analysis

Using the analysis in Sec. IV-A and Sec. IV-B, the favorable channel scenario is given by:  $\mathbf{h}_{ru} \sim \mathcal{CN}(\mathbf{0}, \mathbf{I}_M)$ ,  $\mathbf{h}_d \sim \mathcal{CN}(\mathbf{0}, \mathbf{I}_N)$ . The resulting mean SNR is obtained by substituting the UB of (16) and  $A = \sqrt{M}$  into (9). This gives the very simple result

$$\mathbb{E}\{\text{SNR}_{\text{fav}}\} = \left( \beta_d M + \frac{N\sqrt{M}\pi}{2} \sqrt{\beta_d \beta_{br} \beta_{ru}} + \beta_{br} \beta_{ru} M N^2 \right) \bar{\tau}. \quad (19)$$

Next, we consider the asymptotic gains achievable through increased correlation at the RIS. The relative gain due to correlation can be defined as

$$\text{Gain}_{\text{corr}} = \frac{\mathbb{E}\{\text{SNR}\}_{\text{UB}} - \mathbb{E}\{\text{SNR}\}_{\text{LB}}}{\mathbb{E}\{\text{SNR}\}_{\text{LB}}} \stackrel{(a)}{=} \frac{(4 - \pi)N^2 + (\pi - 4)N}{\pi N^2 + (4 - \pi)N + \frac{4\beta_d}{\beta_{br}\beta_{ru}} + \frac{2NA\pi\sqrt{\beta_d}}{M\sqrt{(\beta_{br}\beta_{ru})}}} \quad (20)$$

where (a) involves substituting (17) and (18) and performing simple algebraic manipulations. Therefore, as  $N \rightarrow \infty$ ,

$$\text{Gain}_{\text{max}} = \lim_{N \rightarrow \infty} \text{Gain}_{\text{corr}} = \frac{4 - \pi}{\pi} \approx 27.32\%.$$

Hence, for a large RIS, the maximum gain due to correlation in the UE-RIS Rayleigh channel is approximately 27%.

## V. RESULTS

Here, we present numerical results to verify the analysis in Secs. III and IV. Users were uniformly randomly distributed in a cell of radius  $R_{\text{cell}} = 100$  m, outside an exclusion zone of  $R_{\text{ex}} = 5$  m which surrounds the BS and RIS individually that are located at  $(0, 0)$  and  $(20, 0)$  respectively. The parameter

$A_0$  in (2) was chosen such that the cell-edge average SNR has a medium of 0 dB with  $d_0 = 1$  m for a scenario with  $M = 32$ ,  $N = 64$  and uncorrelated channels  $\mathbf{h}_d, \mathbf{h}_{ru}$ . This gives  $A_0 = 45$  dB. In addition to these parameter values, we set the pathloss exponent  $\gamma = 3.5$ , shadow fading standard deviation  $\sigma_{\text{sf}} = 6$  dB and  $M = 32$ . In order to verify the analysis, a fixed UE position of  $(10, 20)$  was used and the lognormal shadowing for the link gains is set to  $L = 1$ . As stated in Sec. II-A, the steering vectors for  $\mathbf{H}_{br}$  are not restricted to any particular formation. However, for simulation purposes, we will use the VURA model. The  $x, z$  components of the steering vector at the BS are  $\mathbf{a}_{b,x}, \mathbf{a}_{b,z}$  are given by

$$\begin{aligned} & [1, e^{j2\pi d_b \sin(\theta_A) \cos(\omega_A)}, \dots, e^{j2\pi d_b (M_x - 1) \sin(\theta_A) \cos(\omega_A)}]^T, \\ & [1, e^{j2\pi d_b \cos(\theta_A)}, \dots, e^{j2\pi d_b (M_z - 1) \cos(\theta_A)}]^T. \end{aligned}$$

Similarly at the RIS,  $\mathbf{a}_{r,x}, \mathbf{a}_{r,z}$  are defined by,

$$\begin{aligned} & [1, e^{j2\pi d_r \sin(\theta_D) \cos(\omega_D)}, \dots, e^{j2\pi d_r (N_x - 1) \sin(\theta_D) \cos(\omega_D)}]^T, \\ & [1, e^{j2\pi d_r \cos(\theta_D)}, \dots, e^{j2\pi d_r (N_z - 1) \cos(\theta_D)}]^T, \end{aligned}$$

where  $M = M_x M_z$ ,  $N = N_x N_z$ ,  $d_b = 0.5$ ,  $d_r = 0.2$ , where  $d_b$  and  $d_r$  are in wavelength units. The global steering vectors at the BS and RIS are then given by,

$$\mathbf{a}_b = \mathbf{a}_{b,x} \otimes \mathbf{a}_{b,z}, \quad \mathbf{a}_r = \mathbf{a}_{r,x} \otimes \mathbf{a}_{r,z}, \quad (21)$$

where  $\theta_A$  and  $\omega_A$  are azimuth/elevation angles of arrival (AOAs) at the BS and  $\theta_D, \omega_D$  are the corresponding angles of departure (AODs) at the RIS. Note that all of these parameter values and variable definitions are not altered throughout the results and figures, unless specified otherwise.

### A. Approximate CDF for SNR

It is known that the SNR of a wide range of fading channel can be approximately modeled by a mixture gamma distribution [14]. Also, it is well-known that a single gamma approximation is often reasonable for a variable which is the sum of a number of positive random variables, see [10] for example. Motivated by this, we approximate the SNR in (8) by a single gamma variable.

Let the shape parameter of a gamma approximation to the SNR is given by  $k_\gamma = \frac{\mathbb{E}\{\text{SNR}\}^2}{\text{Var}\{\text{SNR}\}}$  and the scale parameter is  $\theta_\gamma = \frac{\text{Var}\{\text{SNR}\}}{\mathbb{E}\{\text{SNR}\}}$  where  $\mathbb{E}\{\text{SNR}\}$  and  $\text{Var}\{\text{SNR}\}$  are given in Sec. III. Using these values of  $k_\gamma, \theta_\gamma$ , the analytical and simulated SNR CDFs are shown in Fig. 2 for the following scenarios;  $N = 64, \rho_{ru} = \rho_d = \{0.1, 0.7, 0.95\}$  and  $N = 256, \rho_{ru} = \rho_d = \{0.1, 0.7, 0.95\}$ . When computing the analytical SNR CDFs, for  $\rho_{ru} = \rho_d = 0$ , (13) and (14) were used and for  $\rho_{ru} = \rho_d \neq 0$ , (9) and (11) were used. As expected, there is a very good agreement between the simulated and analytical SNR CDFs when  $\rho_d = \rho_{ru} = 0$  due to exact average SNR and SNR variance expressions. Increasing the correlation level, causes the CDF agreement to deviate slightly in the low SNR region, especially in the highest correlation scenario. However a good agreement is maintained in the mid-high SNR region. The gamma distribution therefore

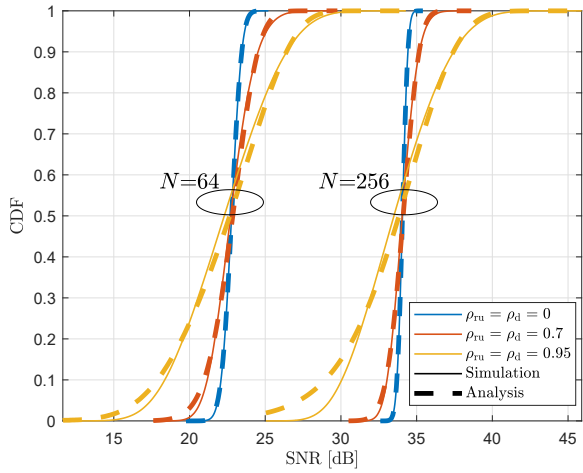


Fig. 2: Simulated and analytical CDFs for following scenarios;  $N = 64, \rho_d = \rho_{ru} = \{0.1, 0.7, 0.95\}$  and  $N = 256, \rho_d = \rho_{ru} = \{0.1, 0.7, 0.95\}$ .

provides a good representation of the UL SNR unless the correlations become very high.

### B. $\rho_d, \rho_{ru}$ and Asymptotic Analysis Results

To verify the analysis of  $\rho_d$ , in Fig. 3 we perform SNR simulations for three different correlation scenarios:  $\rho_{ru} = \rho_d = 0$ ,  $\rho_{ru} = \rho_d = 1$  and the favorable channel scenario  $\rho_{ru} = 1, \rho_d = 0$ . The left subfigure in Fig. 3 shows the

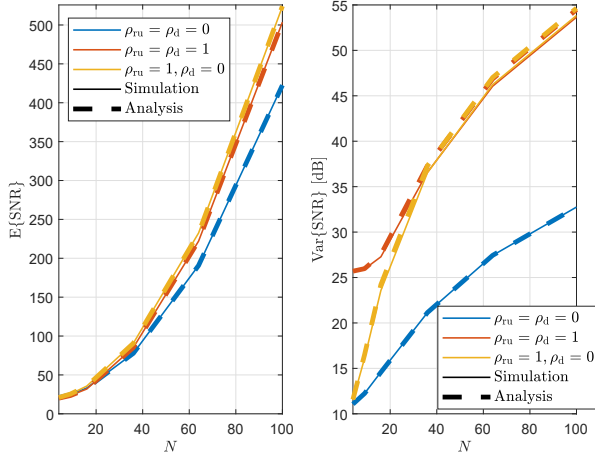


Fig. 3: Simulated and analytical average/variance SNR for three different correlated level scenarios:  $\rho_{ru} = \rho_d = 0$ ,  $\rho_{ru} = \rho_d = 1$  and favorable channel scenario  $\rho_{ru} = 1, \rho_d = 0$ .

quadratic increase in mean SNR as predicted by the analysis. The favorable channel scenario yields the highest mean SNR but the increase over perfect correlation in both channels is marginal. The lowest SNR is when both channels are uncorrelated. Fig. 3 also shows that for all correlation level scenarios, the theoretical analysis agrees with the simulation.

The right subfigure in Fig. 3 shows the accuracy of the SNR variance approximation. There is a perfect agreement for the case where  $\mathbf{h}_{ru}$  and  $\mathbf{h}_d$  are uncorrelated. In the correlated cases, the analysis and simulation agree closely for low  $N$  but begin to deviate slightly as  $N$  grows. This is also reflected in Fig. 2 as the CDF agreement between simulation and analysis is worse for  $N = 256$  compared to  $N = 64$  as  $\rho_d, \rho_{ru} \rightarrow 1$ . Note that the analytical CDFs show a longer lower tail, partially caused by the over-estimate of the variance. As  $N$  grows, observe that the variance for scenarios  $\rho_{ru} = \rho_d = 1$  and  $\rho_{ru} = 1, \rho_d = 0$  converge to approximately the same value. This is because the effects of correlation in  $\mathbf{h}_d$  are reduced by large  $N$ .

Finally, in Fig. 4 we verify the UB, LB by computing the gain due to correlation in  $\mathbf{h}_{ru}$ , and verify the asymptotic analysis in Sec. IV-A and Sec. IV-C. For simplicity, we assume all three channels have the same link gain and let  $\beta_d = \beta_{ru} = \beta_{br} = 1$ . Fig. 4 verifies the analysis in Sec. IV-C

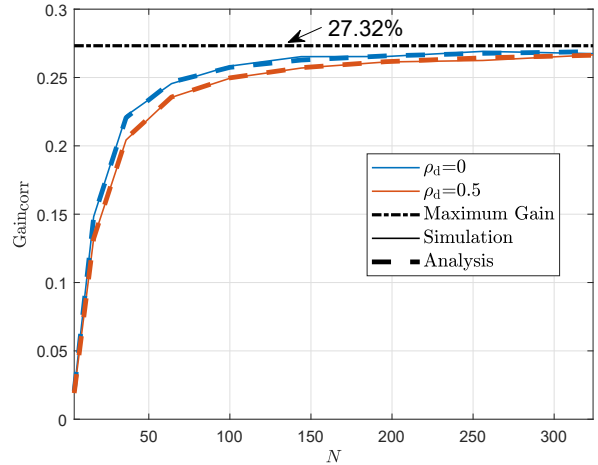


Fig. 4: Average SNR gain due to correlation in  $\mathbf{h}_{ru}$  for varying RIS sizes and correlation in  $\mathbf{h}_d$ .

demonstrating an increasing gain with correlation saturating at approximately 27%. Introducing correlation in the direct channel causes the gain to be lower. However, as explained in the analysis, for large RIS elements, this negative effect is reduced.

The UB and LB given by (17) and (18) respectively are also verified in Fig. 4 as they are used in computing the gain.

## VI. CONCLUSION

In this paper, we derive an exact closed form expression for the mean SNR of the optimal single user RIS design where spatially correlated Rayleigh fading is assumed for the UE-BS and UE-RIS channels and the RIS-BS channel is LOS. We also provide an accurate approximation to the SNR variance and a gamma approximation to the CDF of the SNR. The results also offer insight into how spatial correlation impacts the mean SNR and scenarios in which we would expect high SNR performance.

Substituting the channel vectors and matrices described in Sec. II-A into (8) gives

$$\text{SNR} = \left( \beta_d \mathbf{u}_d^H \mathbf{R}_d \mathbf{u}_d + 2\sqrt{\beta_d} \Re \left\{ \alpha \mathbf{u}_d^H \mathbf{R}_d^{1/2} \mathbf{a}_b \right\} + |\alpha|^2 M \right) \bar{\tau} \\ \triangleq (S_1 + S_2 + S_3) \bar{\tau}.$$

We now compute  $\mathbb{E}\{\text{SNR}\}$  by taking the expectation of each individual term in the above expression.

Term 1: Since  $\mathbf{u}_d \sim \mathcal{CN}(\mathbf{0}, \mathbf{I})$ ,

$$\mathbb{E}\{S_1\} = \beta_d \text{tr}\{\mathbf{R}_d\} = \beta_d M. \quad (22)$$

Term 2: Substituting  $\alpha$  from Sec. II-B we have,

$$\mathbb{E}\{S_2\} = 2\sqrt{\beta_d \beta_{br} \beta_{ru}} \mathbb{E} \left\{ \sum_{n=1}^N \left| \tilde{\mathbf{h}}_{ru,n} \right| \right\} \mathbb{E} \left\{ \left| \mathbf{a}_b^H \mathbf{R}_d^{1/2} \mathbf{u}_d \right| \right\} \\ = 2\sqrt{\beta_d \beta_{br} \beta_{ru}} \mathbb{E}\{Y\} \mathbb{E} \left\{ \left| \mathbf{a}_b^H \mathbf{R}_d^{1/2} \mathbf{u}_d \right| \right\}.$$

Since  $\mathbf{h}_{ru} \sim \mathcal{CN}(\mathbf{0}, \mathbf{R}_{ru})$  it follows that  $\mathbb{E}\{Y\} = \frac{N\sqrt{\pi}}{2}$  [15]. To compute  $\mathbb{E} \left\{ \left| \mathbf{a}_b^H \mathbf{R}_d^{1/2} \mathbf{u}_d \right| \right\}$ , note the following results. As  $\mathbf{u}_d \sim \mathcal{CN}(\mathbf{0}, \mathbf{I}_M)$ , it follows that  $\mathbf{a}_b^H \mathbf{R}_d^{1/2} \mathbf{u}_d$  is zero mean complex Gaussian with

$$\mathbb{E} \left\{ \left| \mathbf{a}_b^H \mathbf{R}_d^{1/2} \mathbf{u}_d \right|^2 \right\} = \left\| \mathbf{R}_d^{1/2} \mathbf{a}_b \right\|_2^2.$$

As such, we have  $\left| \mathbf{a}_b^H \mathbf{R}_d^{1/2} \mathbf{u}_d \right| \sim \frac{1}{\sqrt{2}} \left\| \mathbf{R}_d^{1/2} \mathbf{a}_b \right\|_2 X^{1/2}$  where  $X \sim \chi_2^2$  is a central chi-squared variable. By the moments of a central chi-square distribution with 2 degrees of freedom,

$$\mathbb{E} \left\{ \left| \mathbf{a}_b^H \mathbf{R}_d^{1/2} \mathbf{u}_d \right| \right\} = \left\| \mathbf{R}_d^{1/2} \mathbf{a}_b \right\|_2 \frac{\sqrt{\pi}}{2}. \quad (23)$$

Hence,

$$\mathbb{E}\{S_2\} = \frac{N\pi}{2} \sqrt{\beta_d \beta_{br} \beta_{ru}} \left\| \mathbf{R}_d^{1/2} \mathbf{a}_b \right\|_2. \quad (24)$$

Term 3: Using  $|\psi| = 1$  (where  $\psi$  is given in Sec. II-B) we have  $S_3 = M\beta_{br}\beta_{ru}Y^2$  and expanding  $Y$  gives

$$\mathbb{E}\{Y^2\} = \sum_{i=1}^N \mathbb{E} \left\{ \left| \tilde{\mathbf{h}}_{ru,i} \right|^2 \right\} + \sum_{i=1}^N \sum_{\substack{j=1 \\ i \neq j}}^N \mathbb{E} \left\{ \left| \tilde{\mathbf{h}}_{ru,i} \right| \left| \tilde{\mathbf{h}}_{ru,j} \right| \right\}.$$

Using [15, Eq. (16)], each individual expectation in the double summation is,

$$\mathbb{E} \left\{ \left| \tilde{\mathbf{h}}_{ru,i} \right| \left| \tilde{\mathbf{h}}_{ru,j} \right| \right\} = \frac{\pi}{4} \left( 1 - |\rho_{ij}|^2 \right)^2 {}_2F_1 \left( \frac{3}{2}, \frac{3}{2}, 1; |\rho_{ij}|^2 \right),$$

where  ${}_2F_1(\cdot)$  is the Gaussian hypergeometric function and  $\rho_{ij} = (\mathbf{R}_{ru})_{ij}$ . Using this, we have  $\mathbb{E}\{Y^2\} = N + F$ , where  $F$  is given by (10), giving the final result

$$\mathbb{E}\{S_3\} = \beta_{br}\beta_{ru}M(N + F). \quad (25)$$

Combining (22), (24) and (25) completes the derivation.

To compute the variance we take the square of (8) giving,

$$\text{SNR}^2 = \left( \beta_d^2 (\mathbf{u}_d^H \mathbf{R}_d \mathbf{u}_d)^2 + 4\beta_d^{3/2} \mathbf{u}_d^H \mathbf{R}_d \mathbf{u}_d \Re \left\{ \alpha \mathbf{u}_d^H \mathbf{R}_d^{1/2} \mathbf{a}_b \right\} \right. \\ \left. + 2\beta_d M |\alpha|^2 \mathbf{u}_d^H \mathbf{R}_d \mathbf{u}_d + 4\beta_d \Re \left\{ \alpha \mathbf{u}_d^H \mathbf{R}_d^{1/2} \mathbf{a}_b \right\}^2 \right. \\ \left. + 4\sqrt{\beta_d} M |\alpha|^2 \Re \left\{ \alpha \mathbf{u}_d^H \mathbf{R}_d^{1/2} \mathbf{a}_b \right\} + |\alpha|^4 M^2 \right) \bar{\tau}^2 \\ \triangleq (T_1 + T_2 + T_3 + T_4 + T_5 + T_6) \bar{\tau}^2. \quad (26)$$

Obtaining  $\mathbb{E}\{\text{SNR}^2\}$  is done by performing the expectation of each term in (26).

Term 1: Using [16, Eq. (9)] and  $\mathbf{u}_d \sim \mathcal{CN}(\mathbf{0}, \mathbf{I})$ ,

$$\mathbb{E}\{T_1\} = \beta_d^2 (\text{tr}\{\mathbf{R}_d\} + M^2). \quad (27)$$

Term 2: Expanding the second term gives,

$$\mathbb{E}\{T_2\} = 4\beta_d^{3/2} \sqrt{\beta_{br}\beta_{ru}} Y \mathbf{u}_d^H \mathbf{R}_d \mathbf{u}_d \left| \mathbf{u}_d^H \mathbf{R}_d^{1/2} \mathbf{a}_b \right|, \quad (28)$$

where  $Y$  is defined in Appendix A. To find the expectation of (28), we introduce the following variables: Let  $\mathbf{P}$  be any orthonormal matrix with first column equal to  $\mathbf{p}_1 = \mathbf{R}_d^{1/2} \mathbf{a}_b \left\| \mathbf{R}_d^{1/2} \mathbf{a}_b \right\|_2^{-1}$ . Also let  $\mathbf{x} = \mathbf{P}^H \mathbf{u}_d \sim \mathcal{CN}(\mathbf{0}, \mathbf{I})$  and  $\mathbf{Q} = \mathbf{P}^H \mathbf{R}_d \mathbf{P}$ , then the random component of (28), neglecting  $Y$ , can be rewritten as,

$$\mathbf{u}_d^H \mathbf{R}_d \mathbf{u}_d \left| \mathbf{u}_d^H \mathbf{R}_d^{1/2} \mathbf{a}_b \right| = \mathbf{x}^H \mathbf{Q} \mathbf{x} \left| \mathbf{x}^H \mathbf{P}^H \mathbf{p}_1 \right| \left\| \mathbf{R}_d^{1/2} \mathbf{a}_b \right\|_2 \\ = \mathbf{x}^H \mathbf{Q} \mathbf{x} |x_1| \left\| \mathbf{R}_d^{1/2} \mathbf{a}_b \right\|_2, \quad (29)$$

since  $\mathbf{P}^H \mathbf{p}_1 = [1, \mathbf{0}_{M-1}]^T$ . Note that,

$$\mathbb{E}\{\mathbf{x}^H \mathbf{Q} \mathbf{x} |x_1|\} = \mathbb{E} \left\{ \sum_{i=1}^M \sum_{j=1}^M \mathbf{Q}_{i,j} x_i^* x_j |x_1| \right\} \\ = \mathbf{Q}_{1,1} \mathbb{E}\{|x_1|^3\} + (\text{tr}\{\mathbf{Q}\} - \mathbf{Q}_{1,1}) \mathbb{E}\{|x_1|\} \\ = \frac{\sqrt{\pi} \mathbf{a}_b^H \mathbf{R}_d \mathbf{a}_b}{4 \left\| \mathbf{R}_d^{1/2} \mathbf{a}_b \right\|_2^2} + M \frac{\sqrt{\pi}}{2}$$

since  $\mathbb{E}\{|x_1|\} = \sqrt{\pi}/2$ ,  $\mathbb{E}\{|x_1|^3\} = 3\sqrt{\pi}/4$ ,  $\text{tr}\{\mathbf{Q}\} = \text{tr}\{\mathbf{R}_d\} = M$  and  $\mathbf{Q}_{1,1} = \mathbf{p}_1^H \mathbf{R}_d \mathbf{p}_1 = \frac{\mathbf{a}_b^H \mathbf{R}_d \mathbf{a}_b}{\mathbf{a}_b^H \mathbf{R}_d \mathbf{a}_b}$ . Using the above result and the result for  $\mathbb{E}\{Y\}$  in Appendix A, the expectation of (28) is

$$\mathbb{E}\{T_2\} = \beta_d^{3/2} \sqrt{\beta_{br}\beta_{ru}} N B \pi, \quad (30)$$

where  $B = MA + \mathbf{a}_b^H \mathbf{R}_d \mathbf{a}_b / 2A$  and  $A = \left\| \mathbf{R}_d^{1/2} \mathbf{a}_b \right\|_2$ . The variables  $B$  and  $A$  will be used throughout the proceeding derivation.

Term 3: The expectation of term 3 is,

$$\mathbb{E}\{T_3\} = 2\beta_d \beta_{br} \beta_{ru} M \mathbb{E}\{Y^2\} \mathbb{E}\{\mathbf{u}_d^H \mathbf{R}_d \mathbf{u}_d\} \\ = 2\beta_d \beta_{br} \beta_{ru} M^2 (N + F), \quad (31)$$

where  $\mathbb{E}\{Y^2\}$  is computed in Appendix A.

Term 4: The expectation of term 4 is,

$$\begin{aligned}\mathbb{E}\{T_4\} &= 4\beta_d\beta_{br}\beta_{ru}\mathbb{E}\{Y^2\}\mathbb{E}\left\{\left|\mathbf{a}_b^H\mathbf{R}_d^{1/2}\mathbf{u}_d\right|^2\right\} \\ &= 4\beta_d\beta_{br}\beta_{ru}(N+F)\left\|\mathbf{R}_d^{1/2}\mathbf{a}_b\right\|_2^2,\end{aligned}\quad (32)$$

where  $\mathbb{E}\{Y^2\}$  and  $\mathbb{E}\left\{\left|\mathbf{a}_b^H\mathbf{R}_d^{1/2}\mathbf{u}_d\right|^2\right\}$  are computed in Appendix A.

Term 5: Expanding term 5,

$$T_5 = 4M\sqrt{\beta_d}(\beta_{br}\beta_{ru})^{3/2}Y^3\left|\mathbf{a}_b^H\mathbf{R}_d^{1/2}\mathbf{u}_d\right|.$$

The variable  $Y^3$  is a sum of products of the magnitudes of three correlated complex Gaussian random variables. To the best of our knowledge the mean of such terms is intractable without the use of multiple summations and special functions. As such we will use an approximation based on the gamma distribution to approximate the expectation (see Appendix C). Substituting this approximation and the result for  $\mathbb{E}\left\{\left|\mathbf{a}_b^H\mathbf{R}_d^{1/2}\mathbf{u}_d\right|\right\}$  from Appendix A, we have,

$$\mathbb{E}\{T_5\} \approx 2M\sqrt{\pi}\sqrt{\beta_d}(\beta_{br}\beta_{ru})^{3/2}\left\|\mathbf{R}_d^{1/2}\mathbf{a}_b\right\|_2 C_1, \quad (33)$$

with  $C_1 = b^3a\prod_{k=1}^2(k+a)$  where  $a$  and  $b$  are defined in Appendix C.

Term 6: Expanding term 6,

$$T_6 = (M\beta_{br}\beta_{ru})^2Y^4.$$

Since  $Y^4$  is even more complex than  $Y^3$  we re-use the gamma approximation for  $Y$  to make progress. Using the approximation for  $\mathbb{E}\{Y^4\}$  in Appendix C gives,

$$\mathbb{E}\{T_6\} \approx (M\beta_{br}\beta_{ru})^2 C_2, \quad (34)$$

with  $C_2 = b^4a\prod_{k=1}^3(k+a)$  where  $a$  and  $b$  are defined in Appendix C.

Using (27), (30), (31), (32), (33) and (34) for  $\mathbb{E}\{\text{SNR}^2\}$  and subtracting  $\mathbb{E}\{\text{SNR}\}^2$  completes the derivation after some algebraic simplification

#### APPENDIX C

##### APPROXIMATIONS FOR $\mathbb{E}\{Y^3\}$ AND $\mathbb{E}\{Y^4\}$

Due to  $Y$  being positive and unimodal, we propose approximations for  $\mathbb{E}\{Y^3\}$  and  $\mathbb{E}\{Y^4\}$  using a gamma distribution as an approximation for  $Y$ . From Appendix A, we know that  $\mathbb{E}\{Y\} = N\sqrt{\pi}/2$  and  $\mathbb{E}\{Y^2\} = N+F$ , where  $F$  is defined by (10). Then, the variance of  $Y$  is  $\text{Var}\{Y\} = N+F - \frac{N^2\pi}{4}$ . Using the method of moments, the parameters that define a gamma distribution fit for  $Y$  are,

$$\begin{aligned}a &= \frac{\mathbb{E}\{Y\}^2}{\text{Var}\{Y\}} = \frac{N^2\pi}{4(N+F) - N^2\pi} \\ b &= \frac{\text{Var}\{Y\}}{\mathbb{E}\{Y\}} = \frac{2}{N\sqrt{\pi}}\left(N+F - \frac{N^2\pi}{4}\right),\end{aligned}$$

where  $a$  and  $b$  are the shape and scale parameters respectively. Suppose  $X \sim \mathcal{G}(a, b)$ , then the 3<sup>rd</sup> and 4<sup>th</sup> moments are

$$\mathbb{E}\{X^3\} = b^3a\prod_{k=1}^2(k+a), \quad \mathbb{E}\{X^4\} = b^4a\prod_{k=1}^3(k+a).$$

Substituting  $a$  and  $b$  into the above moments yields the results for  $C_1, C_2$  in Sec. III-A.

#### APPENDIX D

##### $C_{u1}, C_{u2}$ DERIVATIONS FOR $\text{VAR}\{\text{SNR}\}$ IN SEC. III-B

For uncorrelated Rayleigh channels, we derive an exact formulation for  $C_{u1} = \mathbb{E}\{Y^3\}$  and  $C_{u2} = \mathbb{E}\{Y^4\}$ .

##### A. $C_{u1}$ for Uncorrelated Rayleigh

Expanding  $Y^3$ ,

$$\begin{aligned}Y^3 &= \sum_{i=1}^N \left|\tilde{\mathbf{h}}_{ru,i}\right|^3 + \sum_{i=1}^N \sum_{j=1}^N \sum_{k=1}^N \left|\tilde{\mathbf{h}}_{ru,i}\right| \left|\tilde{\mathbf{h}}_{ru,j}\right| \left|\tilde{\mathbf{h}}_{ru,k}\right| \\ &\quad + 3 \sum_{i=1}^N \sum_{j=1}^N \left|\tilde{\mathbf{h}}_{ru,i}\right|^2 \left|\tilde{\mathbf{h}}_{ru,j}\right|.\end{aligned}$$

Since  $\tilde{\mathbf{h}}_{ru} \sim \mathcal{CN}(\mathbf{0}, \mathbf{I}_N)$ , it follows that

$$\begin{aligned}\mathbb{E}\{Y^3\} &= \frac{N3\sqrt{\pi}}{4} + N(N-1)(N-2)\left(\frac{\sqrt{\pi}}{2}\right)^3 \\ &\quad + \frac{3}{2}N(N-1)\sqrt{\pi} \\ &= \frac{N\sqrt{\pi}}{2}\left(\frac{\pi}{4}\prod_{k=1}^2(N-k) + 3N - \frac{3}{2}\right).\end{aligned}\quad (35)$$

##### B. $C_{u2}$ for Uncorrelated Rayleigh

Expanding  $Y^4$ ,

$$\begin{aligned}Y^4 &= \sum_{i=1}^N \left|\tilde{\mathbf{h}}_{ru,i}\right|^4 + 6 \sum_{i=1}^N \sum_{j=1}^N \sum_{k=1}^N \left|\tilde{\mathbf{h}}_{ru,i}\right|^2 \left|\tilde{\mathbf{h}}_{ru,j}\right| \left|\tilde{\mathbf{h}}_{ru,k}\right| \\ &\quad + 3 \sum_{i=1}^N \sum_{j=1}^N \left|\tilde{\mathbf{h}}_{ru,i}\right|^2 \left|\tilde{\mathbf{h}}_{ru,j}\right|^2 + 4 \sum_{i=1}^N \sum_{j=1}^N \left|\tilde{\mathbf{h}}_{ru,i}\right|^3 \left|\tilde{\mathbf{h}}_{ru,j}\right| \\ &\quad + \sum_{i=1}^N \sum_{j=1}^N \sum_{k=1}^N \sum_{m=1}^N \left|\tilde{\mathbf{h}}_{ru,i}\right| \left|\tilde{\mathbf{h}}_{ru,j}\right| \left|\tilde{\mathbf{h}}_{ru,k}\right| \left|\tilde{\mathbf{h}}_{ru,m}\right|.\end{aligned}$$

Since  $\tilde{\mathbf{h}}_{\text{ru}} \sim \mathcal{CN}(\mathbf{0}, \mathbf{I}_N)$ , it follows that

$$\begin{aligned} \mathbb{E}\{Y^4\} &= 2N + N(N-1)(N-2)(N-3)\frac{\pi^2}{2^4} \\ &\quad + 3N(N-1) + 4N(N-1)\frac{3\pi}{8} \\ &\quad + \frac{6\pi}{4}N(N-1)(N-2) \\ &= 2N + \binom{N}{2} \left( \prod_{k=2}^3 (N-k)\frac{\pi^2}{8} + 6 + 3\pi(N-1) \right). \end{aligned} \quad (36)$$

## REFERENCES

- [1] K. Ying, Z. Gao, S. Lyu, Y. Wu, H. Wang, and M. Alouini, "GMD-based hybrid beamforming for large reconfigurable intelligent surface assisted millimeter-wave massive MIMO," *IEEE Access*, vol. 8, pp. 19 530–19 539, 2020.
- [2] Ö. Özdogan, E. Björnson, and E. G. Larsson, "Using intelligent reflecting surfaces for rank improvement in MIMO communications," in *IEEE International Conference on Acoustics, Speech and Signal Processing (ICASSP)*, 2020, pp. 9160–9164.
- [3] Q. Nadeem, A. Kammoun, A. Chaaban, M. Debbah, and M. Alouini, "Asymptotic max-min SINR analysis of reconfigurable intelligent surface assisted MISO systems," *IEEE Transactions on Wireless Communications*, pp. 1–1, 2020.
- [4] H. Yu, H. D. Tuan, A. A. Nasir, T. Q. Duong, and H. V. Poor, "Joint design of reconfigurable intelligent surfaces and transmit beamforming under proper and improper Gaussian signaling," *IEEE Journal on Selected Areas in Communications*, pp. 1–1, 2020.
- [5] Q. Wu and R. Zhang, "Intelligent reflecting surface enhanced wireless network via joint active and passive beamforming," *IEEE Transactions on Wireless Communications*, vol. 18, no. 11, pp. 5394–5409, 2019.
- [6] Q. Nadeem, H. Alwazani, A. Kammoun, A. Chaaban, M. Debbah, and M. Alouini, "Intelligent reflecting surface-assisted multi-user MISO communication: Channel estimation and beamforming design," *IEEE Open Journal of the Communications Society*, vol. 1, pp. 661–680, 2020.
- [7] G. Yu, X. Chen, C. Zhong, D. W. K. Ng, and Z. Zhang, "Design, analysis and optimization of a large intelligent reflecting surface aided B5G cellular internet of things," *IEEE Internet of Things Journal*, pp. 1–1, 2020.
- [8] J. Zhang, J. Liu, S. Ma, C. Wen, and S. Jin, "Transmitter design for large intelligent surface-ssisted MIMO wireless communication with statistical CSI," in *IEEE International Conference on Communications Workshops (ICC Workshops)*, 2020, pp. 1–5.
- [9] M. Jung, W. Saad, M. Debbah, and C. S. Hong, "Asymptotic optimality of reconfigurable intelligent surfaces: Passive beamforming and achievable rate," in *IEEE International Conference on Communications (ICC)*, 2020, pp. 1–6.
- [10] N. N. Kundu and M. R. McKay, "RIS-Assisted MISO Communication: Optimal Beamformers and Performance Analysis," *arXiv preprint arXiv:2007.08309v1*, 2020. [Online]. Available: <https://arxiv.org/abs/2007.08309v1>
- [11] Q. Tao, J. Wang, and C. Zhong, "Performance analysis of intelligent reflecting surface aided communication systems," *IEEE Communications Letters*, pp. 1–1, 2020.
- [12] A. A. Boulogeorgos and A. Alexiou, "Performance analysis of reconfigurable intelligent surface-assisted wireless systems and comparison with relaying," *IEEE Access*, vol. 8, pp. 94 463–94 483, 2020.
- [13] M. Abramowitz and I. A. Stegun, *Handbook of Mathematical Functions with Formulas, Graphs, and Mathematical Tables*. Dover, 1964.
- [14] S. Atapattu, C. Tellambura, and H. Jiang, "A mixture Gamma distribution to model the SNR of wireless channels," *IEEE Transactions on Wireless Communications*, vol. 10, no. 12, pp. 4193–4203, 2011.
- [15] S. Li, P. J. Smith, P. A. Dmochowski, and J. Yin, "Analysis of analog and digital MRC for distributed and centralized MU-MIMO systems," *IEEE Transactions on Vehicular Technology*, vol. 68, no. 2, pp. 1948–1952, 2019.
- [16] H. Tataria, P. J. Smith, A. F. Molisch, S. Sangodoyin, M. Matthaiou, P. A. Dmochowski, J. Zhang, and R. S. Thoma, "Spatial correlation variability in multiuser systems," in *IEEE International Conference on Communications (ICC)*, 2018, pp. 1–7.